Article:

Chatter avoidance in the milling of thin floors with bull-nose end mills: Model and stability diagrams

Campa, F.J.; Lopez de Lacalle, L.N.; Celaya, A.

International Journal of Machine Tools and Manufacture 51(1) : 43–53 (2011)

Abstract

The milling of thin parts is a high added value operation where the machinist has to face the chatter problem. The study of the stability of these operations is a complex task due to the changing modal parameters as the part losses mass during the machining and the complex shape of the tools that are used. The present work proposes a methodology for chatter avoidance in the milling of flexible thin floors with a bull-nose end mill. First, a stability model for the milling of compliant systems in the tool axis direction with bull-nose end mills is presented. The contribution is the averaging method used to be able to use a linear model to predict the stability of the operation. Then, the procedure for the calculation of stability diagrams for the milling of thin floors is presented. The method is based on the estimation of the modal parameters of the part and the corresponding stability lobes during the machining. As in thin floor milling the depth of cut is already defined by the floor thickness previous to milling, it is proposed the use of stability diagrams that relate the tool position along the tool-path with the spindle speed. Hence, the sequence of spindle speeds that the tool must have during the milling can be selected. Finally, this methodology has been validated by means of experimental tests.

Keywords: chatter, stability prediction, thin parts milling

1. Introduction

Chatter vibrations are a common problem in the finish milling of thin flexible walls and floors due to the lack of dynamic stiffness. This means that a bad surface finish or even marks appear on the final surface and the part has to be rejected or needs manual finishing. Regenerative chatter in the milling of thin floors has been less studied than the thin wall chatter. It appears when there is a variable component of the chip thickness in the normal direction to the floor surface, that is, when ball-end mills, bull-nose end mills or tools with inserts with a cutting edge lead angle κ below 90º are used. In aeronautical machining, bull-nose end mills are frequently used to leave a fillet radius between thin floors and walls, so dynamic problems arise [1]. Smith and Dvorak [2] proposed the use of a flat end mill with a lead angle of 90º to avoid the chatter and a ball end mill for the fillet radius milling at low spindle speeds, taking advantage of the process damping effect. Other authors propose the combination of an online variation of the spindle speed to more stable speeds with the predetermined increase of the feed speed in the more compliant areas of the piece [3,4]. Spending less time in compliant areas, self-excitation is reduced. Lee *et al.* [5] made an experimental study of the influence of the orientation of a ball end mill with respect to the floor in 5 axis milling to obtain the ones that reduce the floor vibration amplitude and roughness.

Another solution is the use of fixturing: vacuum fixtures, adaptive fixtures using low melting temperature alloys, or automated fixtures [6]. However, frequently these solutions are neither cheap nor flexible. Another solution is the use of actuators to compensate online the deformation and vibration of the part [7], although the mounting and dismounting of the actuator means adding operations for the machinist. Also, the actuator starts working once the harm is done. An alternative, cheaper solution is to

increase the initial thickness to stiffen the part [1]. The higher the bulk of material previous to finish milling, the higher the stiffness of the part, but also it increases the material waste. Nevertheless, there are no criteria to estimate the thickness necessary to provide enough stiffness yet maintaining a reasonable material waste.

Another solution to prevent chatter is the stability analysis by means of mathematical modelling of the process. This is a predictive knowledge-based approach. A huge effort to understand, predict and avoid chatter has been done since the beginnings of the 20th century and especially for the last twenty years [8]. The stability lobes calculation allows the selection of chatter-free axial depths of cut and spindle speeds that maximize the material removal rate. Altintas and Budak proposed a linear model for spindle-tool chatter avoidance using the single-frequency and the multi-frequency methods to solve the stability problem [9,10]. Alternative algorithms such as semi-discretization, temporal finite elements analysis or Chebyshev collocation methods, allow a faster obtention of the flip lobes [11-14]. What is more, these methods can take into account several nonlinearities as the variation of the modal parameters of the system, or the variation of the geometry or the cutting coefficients of the tool. Zatarain *et al.* determined the influence of the helix angle in the milling of flexible systems with an axial depth of cut above the helix height divided by the number of tooth of the tool [15].

The modelling of the milling of thin floors with bull-nose end mills presents three main problems:
- the variation of the modal parameters of the floor
- the similar dynamic stiffness of the part and the tool
- the variable geometry of the cutting edge

Modal parameters are variable in the machining of every flexible part, due to several reasons, see Fig. 1. The first is the material removal which reduces the mass and the stiffness of the part [16,17]. The second is related to the displacement of the tool over the modes of vibration of the part, e.g., when the tool is machining over a nodal point of a mode, that mode is negligible [18]. The third reason is the variation of the modal parameters in the cutting area [19-22]. Depending on the size of the tool and the frequency of the modes that are being excited, this variation means that the dynamic response to each cutting edge impact is different and it can be very influent on the stability lobes.
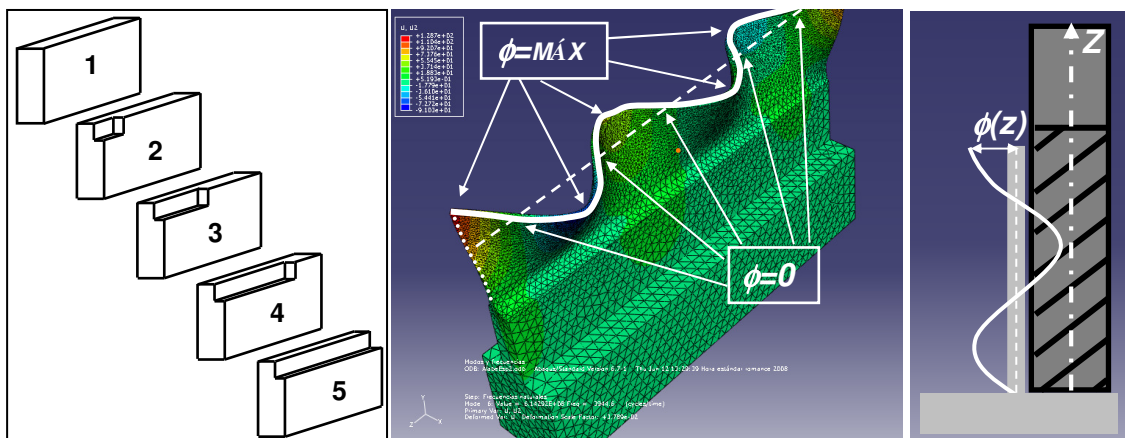

Figure 1. Modal parameters variation in flexible parts milling due to: a) Mass removal. b) Mode shape along the tool-path. c) Mode shape in the cutting area.

In the final stages of the machining, the dynamic stiffness of the thin floor and the tool can be very similar. That means that the combined flexibility of the tool and workpiece has to be taken into account to obtain reliable stability diagrams, instead of considering them separately, as Bravo *et al.* pointed out [23].

The third problem is due to the complex geometry of the bull-nose end mills. When the dominant modes of the system have a low dynamic stiffness in the tool axis direction, i.e. machine-tool modes, thin floor modes, or spatial manipulator modes [24], the value of the cutting edge lead angle has a strong influence on the chatter appearance. The lower the lead angle, the higher is the self-excitation of those modes. [25]. What is more, bull-nose end mills have a variable cutting edge lead angle as well as variable cutting coefficients [26].

In this article the authors propose a method for the improvement of the milling of thin floors with bull-nose end mills by means of the calculation of stability charts. First, the model for milling of compliant systems in the tool axis direction with bull-nose end mills is presented. Then, the method is presented. As a result, a stability diagram that shows how the spindle speed must be varied for a stable milling is obtained. Finally, several experimental tests are made to assess the viability of the method and, to sum up, some conclusions will be presented.

2. Nomenclature

$\phi_j(t)$: Angular position of the cutting edge j measured from axis Y, perpendicular to the feed direction.
h_j: Dynamic chip thickness being cut by a cutting edge j.
F_t, F_r, F_a: Tangential, radial, and axial cutting forces over on cutting edge j.
K_{tc}, K_{rc}, K_{ac}: Shearing cutting coefficients in tangential, radial and axial directions.
$K_r^{'}$, $K_a^{'}$: Ratio of K_{rc}/K_{tc} and K_{ac}/K_{tc}.
$\{F\}$: Dynamic forces vector. Components in X, Y and Z directions.
$\{\Delta\}$: Dynamic displacements vector. Components in X, Y and Z directions.
a_p: Axial depth of cut.
a_e: Radial depth of cut.
ω_c: Chatter frequency.
$[G_{t,w}]$: Frequency response function matrix of the tool or the workpiece.
N: Spindle speed (rpm).
κ: Cutting edge lead angle.
n_h: Number of harmonics of the multi-frequency solution.
n: Number of degrees of freedom of the model.
t: Time.
R: Tool radius.
r_0: Tool corner radius.
f_z: Feed per tooth.

3. Stability model of the milling of flexible systems in the tool axis direction with bull-nose end mills

Bull-nose end mills have a variable diameter and helix angle along the tool axis as well as a variable lead angle, from 0º to 90º, in the toroidal part. In the flank, the lead angle is

constant and equal to 90º [27]. Regarding the mechanistic forces models, the cutting coefficients for these tools are also variable due to the cutting speed and the edge geometry variation along the flute. Lamikiz [26] demonstrated that a linear relation between cutting coefficients and axial depth of cut provides better results than a set of constant coefficients. The relation between those factors and the depth of cut introduces a nonlinearity that has to be solved to calculate the stability lobes diagram using a linear model. In fact, the eigenvalue problem that has to be solved to calculate the stability boundary becomes dependent on the result, the axial depth of cut:

$$\{F\} = a_p \cdot K_{tc}\left(a_p\right) \cdot \left[A\left(\kappa\left(a_p\right), K_{rc}\left(a_p\right), K_{ac}\left(a_p\right)\right)\right] \cdot \left(1 - e^{-i\omega_c T}\right)\left[G\left(\omega_c\right)\right]\{F\} \quad (1)$$

The use of an average value for the cutting coefficients and the cutting edge lead angle can solve this problem. Altintas simplified a circular insert geometry taking an average edge angle of 45º [28]. Abrari *et al.* proposed a method for ball end mills based on the estimation of an average chip thickness and cutting coefficients [29]. Altintas *et al.* proposed the use of an equivalent radial coefficient obtained from the projections of the radial and binormal forces on the XY plane [30]. Then they obtained constant cutting coefficients averaging in the static chip thickness and iterating until completion of the stability diagram. Finally, Budak and Altintas proposed the discretization of the geometry of the tool to consider the stability of several nodes in cut [18]. This method was initially proposed to study the influence of the variation of the modal parameters along the tool axis but it can be applied to varying tool geometries [31]. The main problem of this approach is the computational cost, as it means to solve an eigenvalue problem with a growing size of n, $2n$, $3n$, $4n$, $5n$, in single-frequency solution where n is the DOF of the model. In a multi-frequency solution it means to solve a problem of $n(2n_h+1)$, $2n(2n_h+1)$, $3n(2n_h+1)$, $4n(2n_h+1)$, $5n(2n_h+1)$ order, where n_h is the number of harmonics considered.

3.1 Basics of the linear model

The milling model size can be varied depending on the case: one-dimensional in the tool axis direction for thin floors milling and three-dimensional for stability of the milling with a flexible tool, wall and floor. Although the model is explained in [32], the basics are shown here. First, the following hypotheses have been assumed:
- Cutting forces are modelled by means of a mechanistic model where the tangential, radial and axial forces depend linearly on the chip thickness and the depth of cut [33].
- The helix angle is neglected since it is very low for bull-nose end mills compared to the depths of cut that can be used. Hence, no effect of the helix angle on the stability lobes is expected.
- Nonlinearities as the process damping, loss of contact between cutting edge and workpiece, or multi-regenerative effects are neglected.
- The modal parameters of the system are assumed to be constant inside the cutting area.

Additional assumptions for the milling of systems with low dynamic stiffness in the tool axis direction have been made:
- Only the tool primary cutting edge cuts. When a floor vibrates toward the tool, the secondary edge may become the main one, like in a drilling operation, but it is considered that this effect will only be noticeable in unstable conditions.

- The cutting edges outside the cutting area may interfere with the workpiece too. This backcutting effect is again assumed to be noticeable only when chatter appears, so it will be neglected.
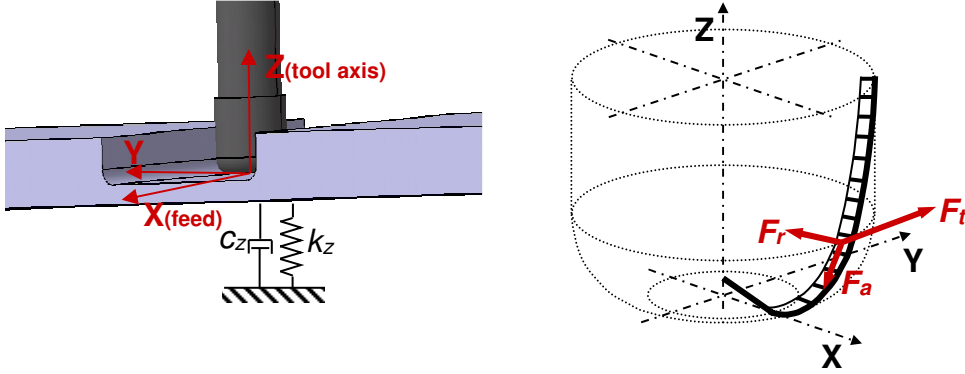

Figure 2. Left) Axis used on the model. Right) Orientation of the cutting forces on an infinitesimal portion of the cutting edge.

Figure 2 indicates the axis assumed for the model and the orientation of the cutting forces over the cutting edge. The dynamic forces acting on the cutting edge are:

$$\begin{Bmatrix} F_t(t) \\ F_r(t) \\ F_a(t) \end{Bmatrix} = K_{tc} \cdot a_p \begin{Bmatrix} 1 \\ K_r' \\ K_a' \end{Bmatrix} h_{d_j}(t) \tag{2}$$

Where h_{dj} is the dynamic chip thickness that the edge j removes. The static chip thickness is considered to be negligible regarding the regenerative effect:

$$h_{d_j}(t) = \left[\left(\Delta x(t) \cdot \sin \phi_j(t) + \Delta y(t) \cdot \cos \phi_j(t) \right) \cdot \sin \kappa - \Delta z(t) \cdot \cos \kappa \right] \cdot g(t) \tag{3}$$

By means of a rotation matrix, the forces in Cartesian coordinates are obtained. Introducing Eq. 3 in Eq. 2, dynamic forces and dynamic displacements can be related by the matrix of the directional factors.

$$\begin{Bmatrix} F_x(t) \\ F_y(t) \\ F_z(t) \end{Bmatrix} = a_p \cdot K_{tc} \left[A(t) \right] \begin{Bmatrix} \Delta x(t) \\ \Delta y(t) \\ \Delta z(t) \end{Bmatrix} \tag{4}$$

Starting from Eq. 4, two stability algorithms have been used depending on the relation between the cutting frequency and the modal frequencies of the system: single-frequency and multi-frequency. These algorithms were developed in [9, 34] to calculate the stability boundary.

3.2 Linearization of the cutting edge lead angle and the cutting coefficients

The nonlinearity due to the variable cutting edge lead angle and cutting coefficients is here solved by means of an averaging iterative procedure. The tool cutting edge is first divided in several sections and, for each one, representative values of the cutting coefficients and the lead angle are calculated by averaging. Then, the corresponding portion of the lobes diagram is calculated. In several iterations, the entire stability lobes diagram can be assembled. The procedure is represented in Figure 3.
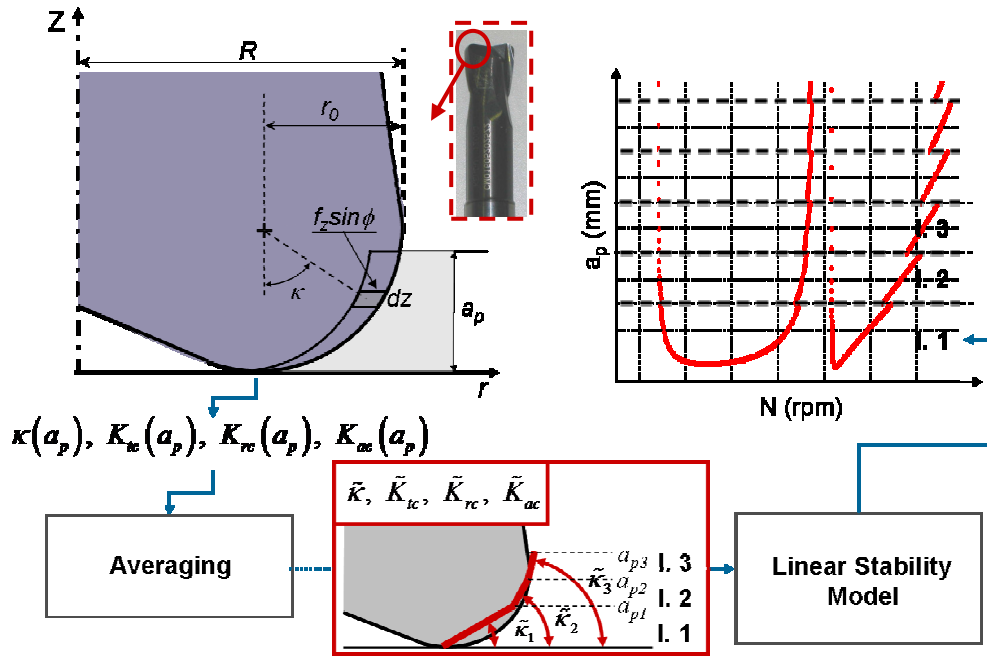
Figure 3. Iterative averaging procedure and bull-nose end mill geometrical parameters.

On the other hand, when a bull-nose end mill is used in a system that is only flexible in the tool axis direction, the regeneration only happens in the toroidal part, see Fig. 4 left. The flank of the tool does not contribute to the chip thickness modulation. That is the reason why the averaging of the edge lead angle and the cutting coefficients is made in the dynamic chip volume, instead of averaging in the static volume, as it is the dynamic chip thickness modulation the responsible for the chatter appearance. So, the proposed equation for the averaging of the cutting edge lead angle, the same would be for the cutting coefficients, is:

$$\tilde{\kappa} = \frac{1}{V_{din}} \int_V \kappa \cdot dV = \frac{1}{V_{din}} \int_S \kappa \cdot h_d(\phi, \kappa)\, dS \tag{5}$$

Where the dynamic chip thickness depends on the radial Δr and axial Δz displacement, see Fig. 4:

$$h_d(\phi, \kappa) = \Delta r \cdot \sin \kappa - \Delta z \cdot \cos \kappa \tag{6}$$
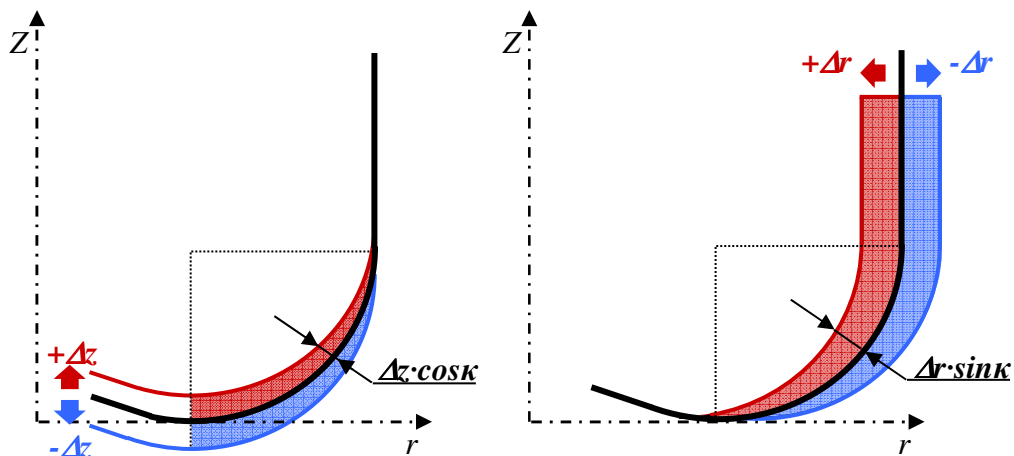

Figure 4. Influence of the axial (left) and radial (right) dynamic displacements on the section of the dynamic chip volume.

Thus, Eq. 5 can be then represented as:

$$\tilde{\kappa} = \frac{\displaystyle\int_{S(\phi,\kappa)} \kappa \cdot (\Delta r \cdot \sin \kappa - \Delta z \cdot \cos \kappa)\, dS(\phi,\kappa)}{\displaystyle\int_{S(\phi,\kappa)} (\Delta r \cdot \sin \kappa - \Delta z \cdot \cos \kappa)\, dS(\phi,\kappa)} \tag{7}$$

However, the magnitude of the dynamic displacements is unknown. When the system is dominantly compliant in axial direction, i.e. a thin floor, radial displacements can be neglected, and vice versa. For thin floors milling, $\Delta r=0$, Eq. 7 can be simplified to:

$$\tilde{\kappa} = \frac{\displaystyle\int_{S(\phi,\kappa)} \kappa \cdot \cos \kappa \cdot r(\kappa) \cdot dS(\phi,\kappa)}{\displaystyle\int_{S(\phi,\kappa)} \cos \kappa \cdot r(\kappa) \cdot dS(\phi,\kappa)} \tag{8}$$

When the compliance in radial and axial direction is similar, the solution proposed is to quantify how compliant it is in each direction. The modal parameters of the system, i.e., the maximum of the FRF, and the mean of the quasi-static cutting forces have been taken into account to obtain a reference value of the mean displacements:

$$\Delta r' = \Delta x' \cdot \sin \phi + \Delta y' \cdot \cos \phi \begin{cases} \Delta x' = \max\left(G_{xx}\right) \cdot \overline{F}_x + \max\left(G_{xy}\right) \cdot \overline{F}_y + \max\left(G_{xz}\right) \cdot \overline{F}_z \\ \Delta y' = \max\left(G_{yx}\right) \cdot \overline{F}_x + \max\left(G_{yy}\right) \cdot \overline{F}_y + \max\left(G_{yz}\right) \cdot \overline{F}_z \end{cases} \tag{9}$$

$$\Delta z' = \max\left(G_{zx}\right) \cdot \overline{F}_x + \max\left(G_{zy}\right) \cdot \overline{F}_y + \max\left(G_{zz}\right) \cdot \overline{F}_z$$

As a result, more weight is given to the $\sin \kappa$ or the $\cos \kappa$ in the Eq. 7, thus considering if the system is dominantly flexible in a given direction and also if the cutting forces excite that direction.

Toroidal part			Flank		
K_{rc}	K_{tc}	K_{ac}	K_{rc}	K_{tc}	K_{ac}
$558,35-198,93 \cdot z$	$1723,3-369,44 \cdot z$	$48,26+52,15 \cdot z$	$65,4$	$804,7$	174

Table 1. Cutting coefficients of the tool in N/mm^2.

Figure 5 shows the real values of the cutting edge lead angle and the cutting coefficients along the tool flute. In comparison, the averaged values are shown when the system is flexible only in axial direction ($\Delta r=0$), when the system is flexible only in radial direction ($\Delta z=0$) and when the system is equally flexible in both directions. The averaging gives more weight to the values of the part of the tool where the modulation of the dynamic chip thickness dominates, as it has been illustrated in Fig. 4. The real cutting coefficients are shown in Table 1. They have been experimentally measured using a Kistler 9255B dynamometric table and a Kistler 5017B amplifier connected to an Oros OR35 signal analyzer. The procedure followed to calculate them as a function of the depth of cut and then validate them is shown in [26].
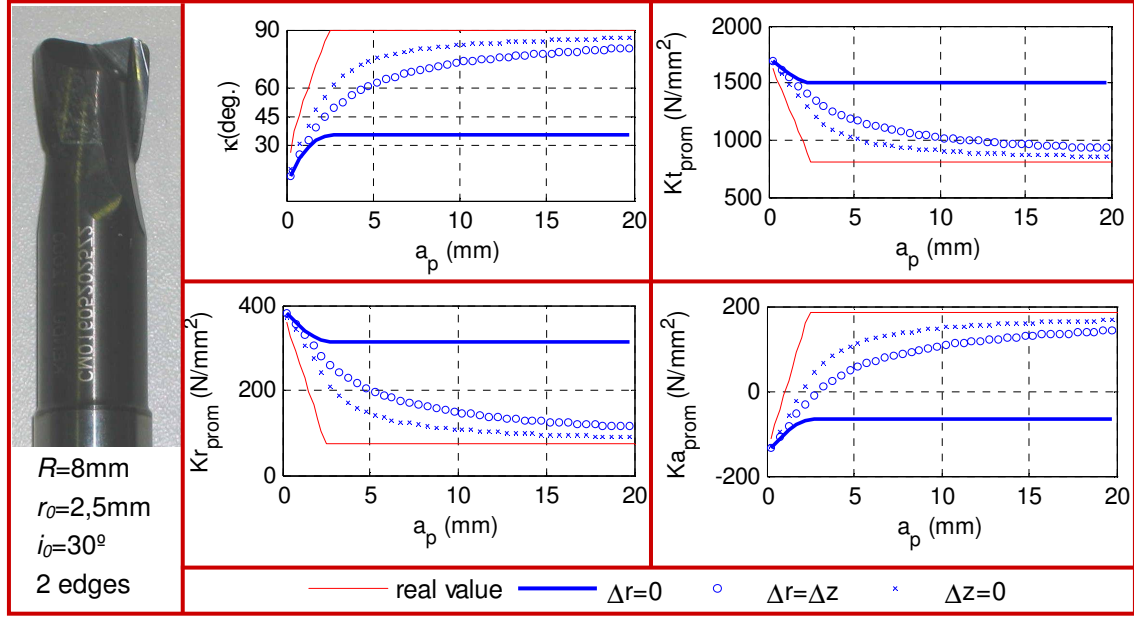
Figure 5. Tool characteristics. Real and the averaged values of the edge lead angle and the cutting coefficients when the dynamic displacements are: Δr=0, Δr=Δz, Δz=0.

4. Calculation of stable spindle speeds for thin floors milling

This work assumes the methodology originally proposed for thin walls milling by Thevenot *et al.* [35], but a different stability diagram is proposed. The method follows these steps:

- Discretization of the toolpath
- Modal parameters calculation by FEM
- Stability diagram representation

4.1 Tool-path discretization

The most critical steps of the machining have to be selected to generate the geometry for the FEM analysis. The geometry of the part depends on the initial geometry, the material that has been removed, the geometry of the tool and the radial and axial steps selected.

4.2. FEM modal analysis

Although there is some variation, it is assumed that the modal parameters are constant in the cutting area. Hence, the most conservative ones, the most flexible, are selected. The steps to obtain the frequency response functions (FRF) are the following, as it is shown in Fig. 6:

1. *FEM modal analysis of the floor and effective stiffness calculation:* Once the modal frequencies ω_m and the modal matrix $[\phi]$ are obtained, the contribution of the dominant modes to the total dynamic stiffness where the tool excites the part is:

$$k_{im} = \frac{\omega_m^2}{\{\phi_i\}_m^2} \tag{10}$$

Where k_{im} is the effective stiffness of the mode m at the point i of the model of the part [36].

2. *Experimental impact tests:* The damping is obtained by modal fitting of impact hammer tests performed on the part. Figure 5 shows the distribution of the measured damping ratio for the test part used in this work on a basis of 1.398 modal fittings.

3. *FRF Matrix assembly:* The 9 terms of the FRF matrix can be obtained from the modal frequency f_m, effective stiffness k_m and damping coefficient ξ_m of the n main nodes.

Also, whenever the dynamic stiffness of the part is similar to the stiffness of the tool or machine tool, it is necessary to include the FRF measured at the tool tip.

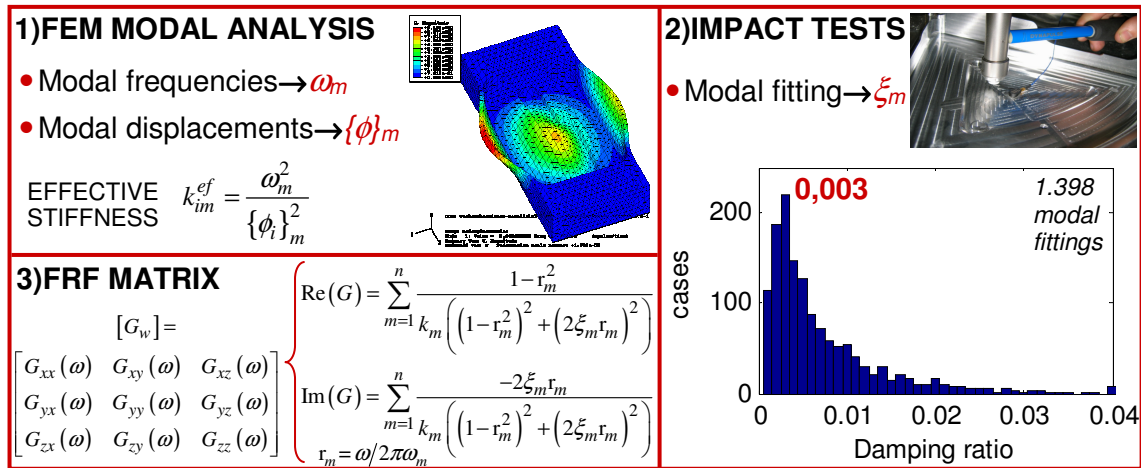$$\left[G(\omega)\right] = \left[G_t(\omega)\right] + \left[G_w(\omega)\right] \tag{11}$$

Figure 6. Steps to estimate the frequency response matrix of the workpiece.

4.3. Stability diagram representation

The three-dimensional stability lobes proposed by Thevenot [35] and Bravo [23] add a third axis to the traditional lobes diagram, the tool position along the tool-path. Hence, it is possible to observe the evolution of the lobes shape during the machining due to the variation of the modal parameters. Nevertheless, this diagram becomes very complex when there is a strong variation in the modal parameters and several lobes appear, making difficult the deduction of stable cutting conditions. On the other hand, the purpose of the stability lobes calculation for thin parts milling is not the selection of an optimal depth of cut as it is done for machine-tool or spindle-tool chatter. In fact, the radial and axial depths of cut are previously selected and used to generate the geometry analyzed by FEM, so the only real variable is the spindle speed.

Hence, it is here proposed the use of the section of the three-dimensional diagram at the depth of cut previously selected for the operation. This diagram relates the spindle speed and the tool position along the tool-path. Figure 7 shows two alternative diagrams for the cut of a three-dimensional diagram at an axial depth of cut of 5 mm. On the left, just the section is shown. The closed areas represent unstable conditions that must be avoided varying the spindle speed along the tool-path, as it is proposed in the figure as an example. On Fig. 7 right, a contour stability diagram is shown. This diagram not only indicates the stable zones, but also provides the limiting depth of cut inside the unstable areas. The chatter severity will not be the same inside those zones, and the contour diagram measures how prone to chatter are those spindle speeds. Whenever the

selection of a stable speed is not possible, the contour diagram can be used to select the less damaging unstable speeds.
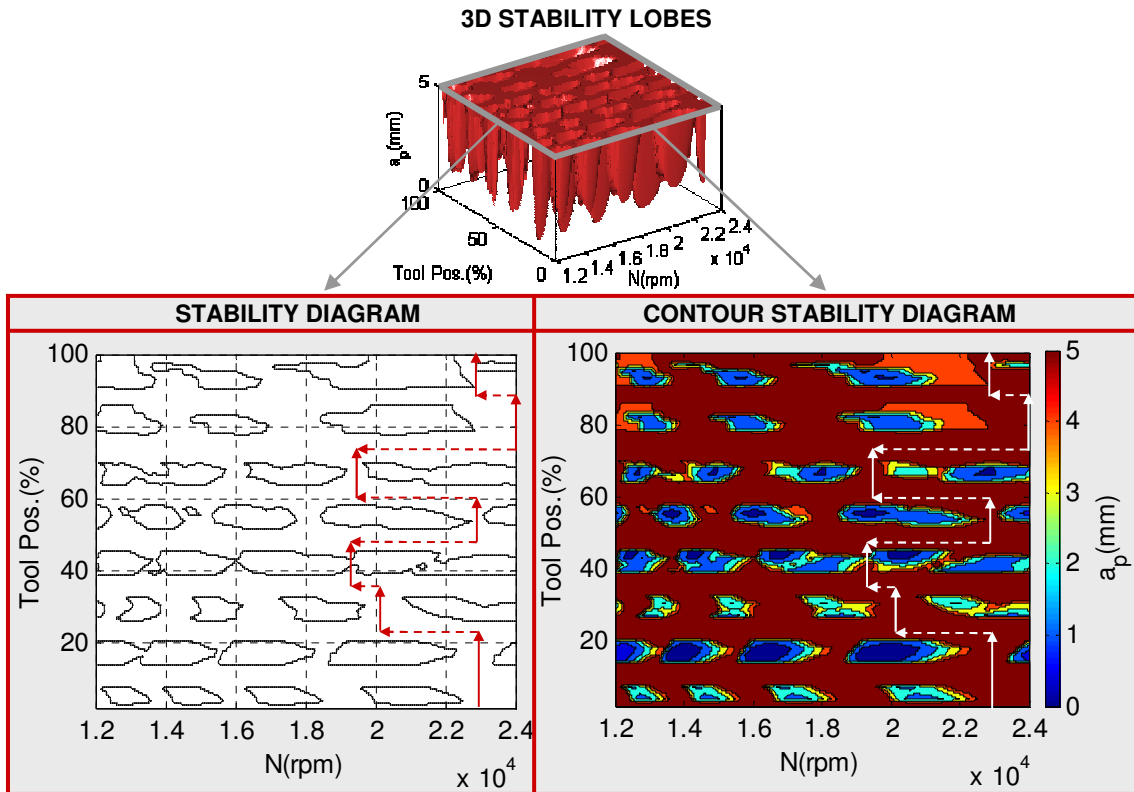

Figure 7. Sections of the 3D stability lobes at a_p=5mm: Stability Diagram (left) and Contour Stability Diagram (right).

6. Experimental Validation

Two setups have been used for validation purposes. The first is used to validate the stability model and the second to validate the stability diagrams for the milling of a thin floor. All the tests have been made with the bull-nose end mill shown in Fig. 5. The machine-tool is a Kondia HS1000 milling centre with a maximum spindle speed of 24000 rpm. The frequency response functions of the experimental devices have been measured using an impact hammer PCB 086C03 and an accelerometer PCB 352C22. Then a modal fitting has been done using the modal analysis toolbox of the CutPro software. The vibration during the milling has been measured using the PCB 352C22 accelerometer glued to the part and a PCB 130D20 microphone. A Fourier analysis of the signals has been done to determine the stability of the milling. An Oros OR35 signal analyzer with 4 channels has been used for these purposes.

6.1 Stability model validation

A block of Aluminum 7075 of 170x112x54 mm over a cantilever plate with an overhang of 120 mm has been used, see Fig. 8 left. The purpose of this setup is to reduce the uncertainty due to the variation of the modal parameters during the milling. Several cutting conditions have been tested in down-milling in X direction from 3.000 to 10.000 rpm and axial depth of cut from 0,5 to 7 mm. The radial depth of cut has been fixed to 2,5 mm as well as the feed per tooth, which has been 0,05 mm.

The dominant mode of the workpiece is a flexural mode whose modal parameters are shown in Fig. 8. The stability lobes have been obtained using the multi-frequency solution. Corresponding to the natural frequency of 111,26 Hz and a tool of 2 cutting edges, there is a clear Hopf lobe in the 3.500 to 6.500 rpm area, and a first order flip lobe in the 7.200 to 10.000 rpm area.
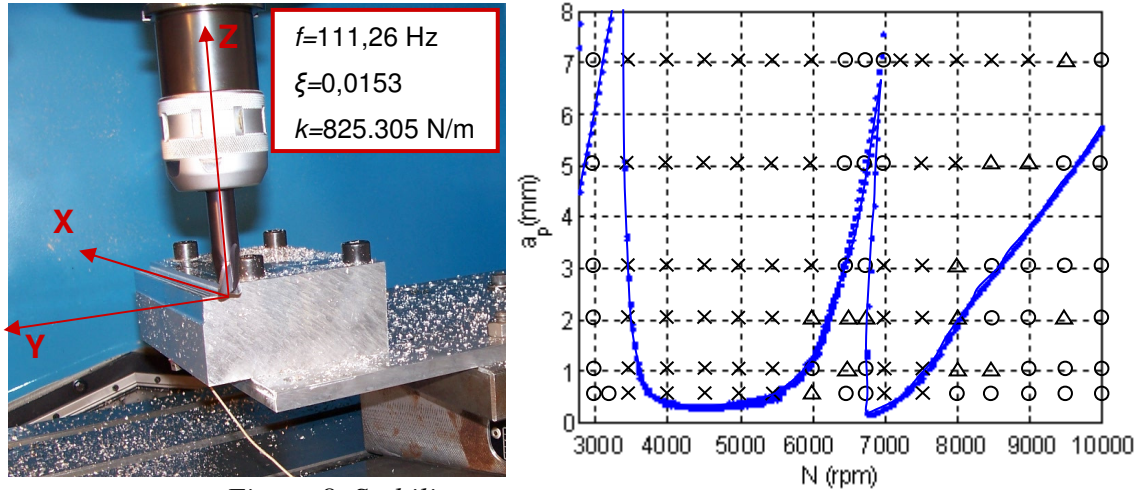

Figure 8. Stability model validation setup and results.

The experimental results are compared in Fig. 8 right. Given the fact that near the stability boundary it becomes difficult to distinguish stable and unstable situations, three cases have been characterized: stable milling (O), unstable milling (×), and slightly unstable (△). Bearing in mind all the simplifications that have been done in the model the results obtained are acceptable, the prediction matches the experimental result in the 87% of the tests. The main discrepancies are located in the right flank of the lobes, where the lobe shape is more sensitive to the errors in the input parameters of the model and the modelling itself.

6.2 Application to a test part

An aluminum pocket with a thin floor without back support has been used for this test, see Fig. 9. The surface finish after milling has been compared. First, milling at 24.000 rpm, the maximum of the machine. Then, varying the spindle speed according to the stability diagram. The objective is to demonstrate that the reduction of the spindle speed from the maximum one makes sense to achieve a better surface finish and productivity [37]. The measurement of the surface finish has been made with a Taylor&Hobson Surftronic+3 after the removal of one end of the part as it is shown in the detail of the Fig. 9 right.

The floor is finish milled to a thickness of 1 mm starting from an initial thickness of 7 mm. An initial value thinner than 6 mm proved to be too flexible to be able to find stable spindle speeds. The milling of the floor has been divided into 8 steps and each of them has been subdivided into 7 steps for the FEM study. The radial depth of cut is 9,67 mm for all the steps but the 1 and 2, which are milled in full immersion. The milling strategy is based on several parallel cuts, as it is shown in Fig. 9, where steps 1 and 2 are the ramp-down of the tool into the workpiece and return to the origin. Hence, the axial depth of cut is variable in steps 1 and 2, and equal to 6 mm in the others. The floor

is cut in down-milling with a feed per tooth of 0,05 mm. The tool used is the bull-nose end mill shown in Fig. 5. No coolant or lubricant has been used.
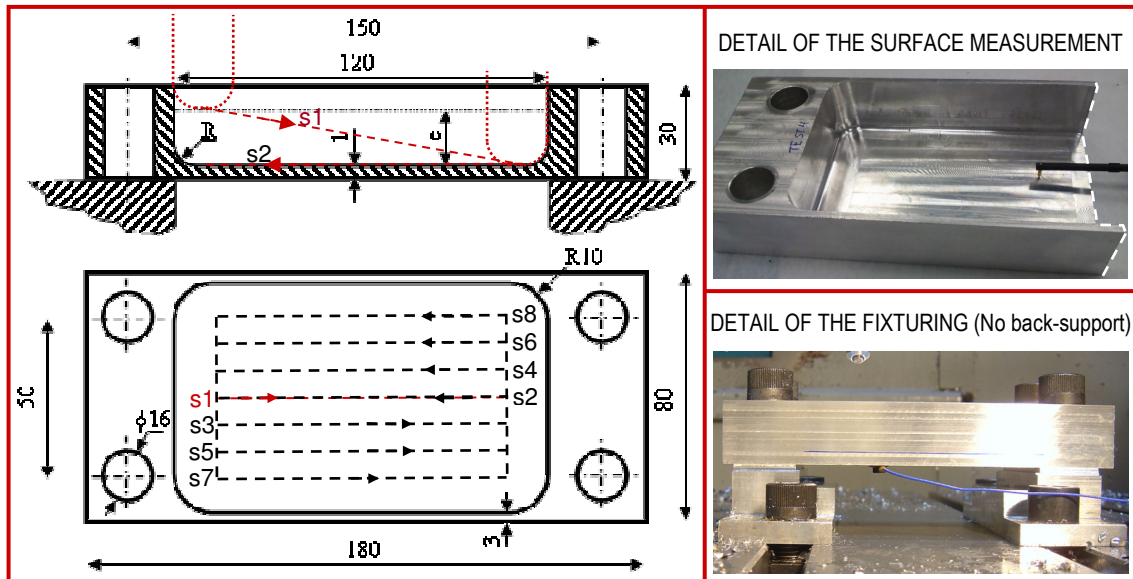

Figure 9. Left) Geometry and dimensions of the test part. Dashed lines illustrate the 'Parallel' strategy tested and the ramp-down milling of the step 1. Right) Details of the surface measurement and the fixturing.

6.2.1 Dynamic response calculation

After the FEM modal analysis, the effective stiffness of all the intermediate positions has been calculated. The damping coefficients obtained with the experimental tests with modal fitting have been applied to the corresponding calculated modes. Figure 10 left shows the evolution along the machining of the FRF module of the floor in the tool excitation point. The main floor modes have a frequency between 2 kHz and 4 kHz and the frequency of the main modes varies about 1 kHz as the floor loses mass during the milling.
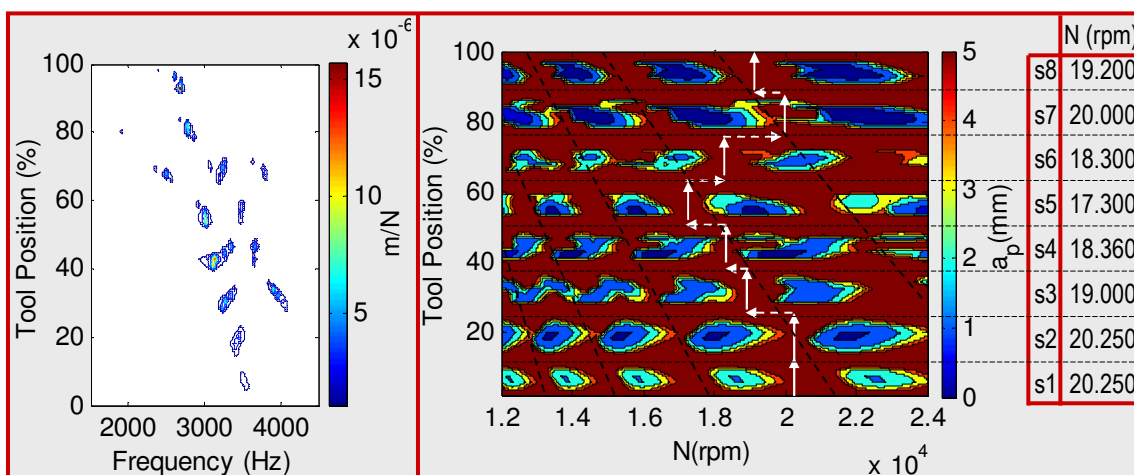

Figure 10. Left.) Evolution of the FRF of the floor. Right.) Stability diagram of the machining of the floor and selected spindle speeds for each step.

6.2.2 Stability diagram

The stability areas evolution along the tool path is shown in Fig. 10 right. The main modal frequencies are between 2 kHz and 4 kHz, and the maximum spindle speed is 24.000 rpm, which means a cutting frequency up to 800 Hz. Hence, the lobes displayed are of third to sixth order. Taking into account also the low dynamic stiffness of the part, the resultant space between unstable areas is narrow, up to 2.000 rpm in the best case. In the worst case, step 7, there is an overlap between lobes that suggest that no stable speed can be found.

The selected spindle speeds for each step in rpm are 20.250-20.250-19.000-18.360-17.300-18.300-20.000-19.200. The selection of the speeds has been made taking into account that the spindle inertia didn't allow abrupt speed variations, so, for example, in step 5 the selected speed was 17.300 to have a smoother transition from step 4. In the step 7, the spindle speed selected crosses the narrowest unstable area. It has to be considered also, that the lobes predicted have an uncertainty due to the errors in the modelling and the errors in the estimation of the modal parameters, so a margin of security in the speed selection is advisable.

6.2.4 Experimental results

Figures 11 and 12 show the surface finish of the part machined at 24.000 rpm and varying the spindle speed. The surface has been divided in sections where the surface characteristics were similar, that is, either they have approximately the same R_a roughness or they are marked due to chatter or forced vibration. The mean R_a roughness in microns is indicated. The step and the direction of milling are indicated in the right side of the figures. After the visual study of the surface and the analysis of the signals, three kinds of phenomena have been observed: the common chatter mark, the ploughings, where the tool suddenly engages the floor penetrating on it, and some long marks. Authors can't associate the last two problems with chatter or a forced vibration problem although they are obviously related to the lack of stiffness.
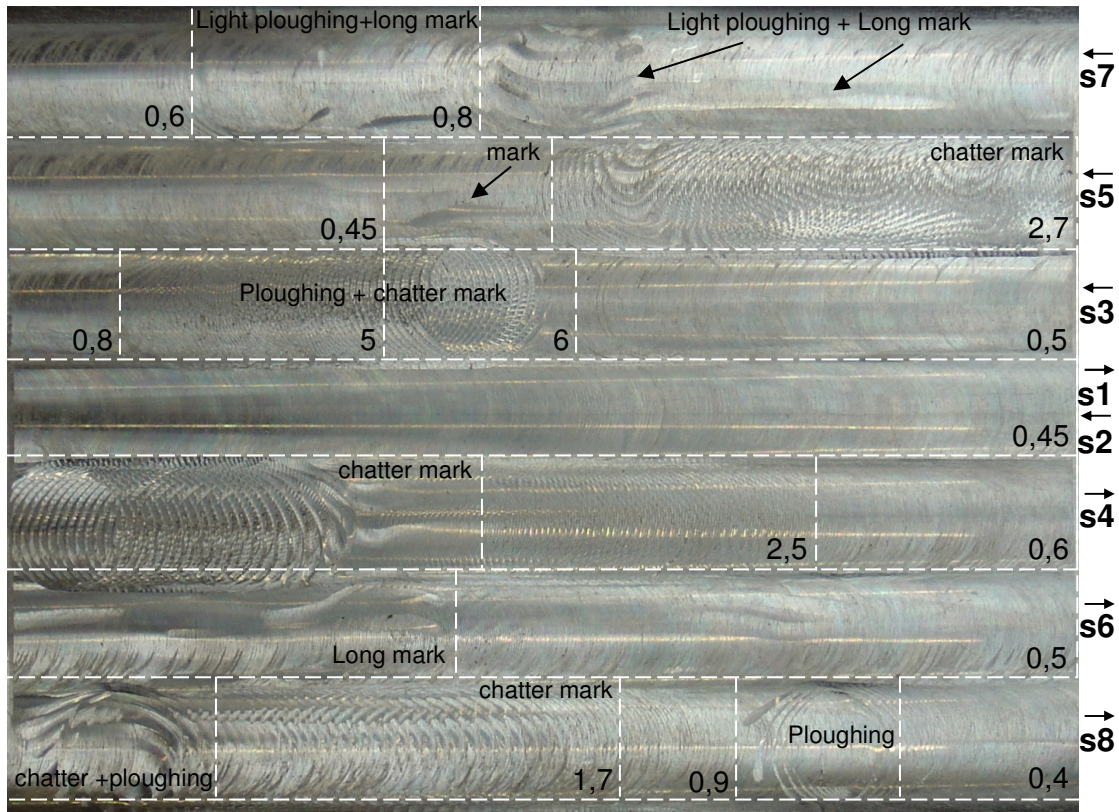
Figure 11. Surface finish (Mean R_a in microns) of the part milled at 24.000 rpm. The tags on the right identify the step and, the arrows, the feed direction of the tool.

Nevertheless, it can be stated that the improvement of the surface finish with the varying spindle speed approach is noticeable in comparison with the test performed at the maximum spindle speed of the machine. Figure 13 shows the mean R_a roughness for the whole surfaces and the standard deviation measured. Not only the mean value has been improved from 1,49 μm to 0,4 μm, but also the deviation has been greatly reduced.
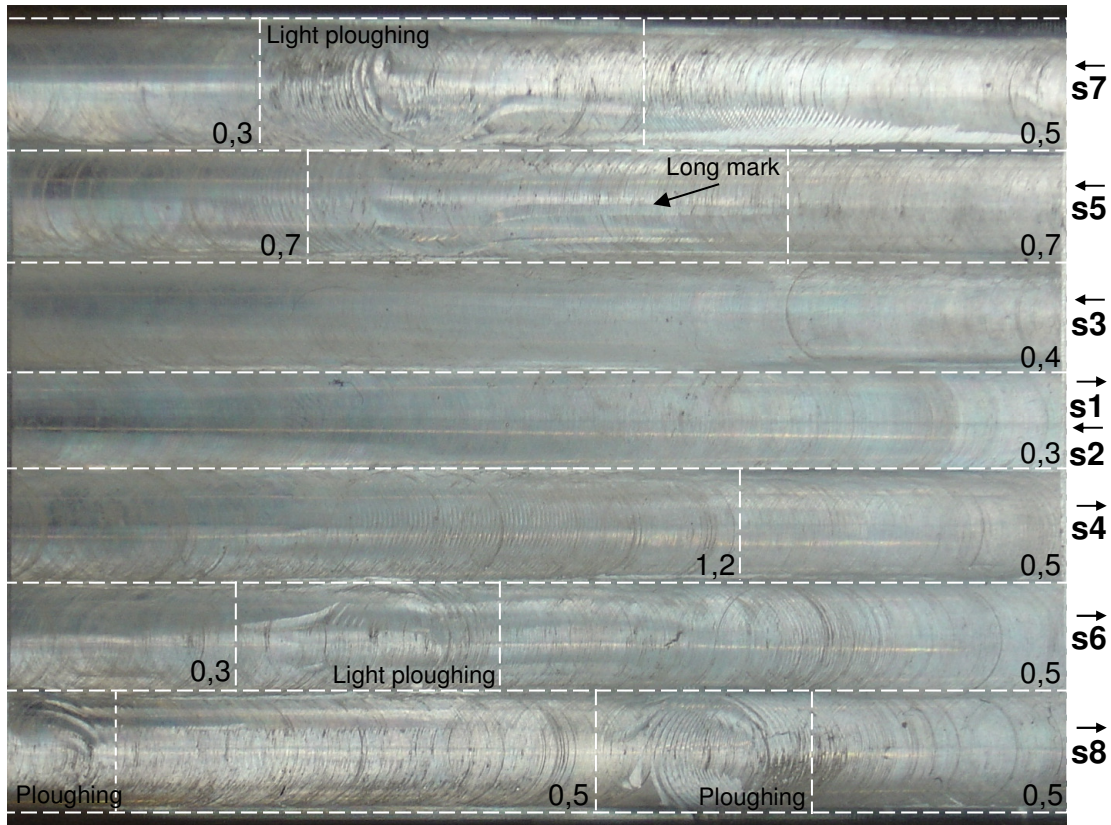
Figure 12. Surface finish (Mean R_a in microns) milling with variable spindle speed. The tags on the right identify the step and, the arrows, the feed direction of the tool.

6.2.4 Discussion

Although the proposed method has improved the surface finish of the test part, the selection of the stable spindle speeds can be difficult. The relation between the modal frequencies of the workpiece and the tooth passing frequencies limits the spindle speeds available to an area between the lobes of third to sixth order, where the stable areas are narrower and more sensitive to error in the input parameters or the modelling.
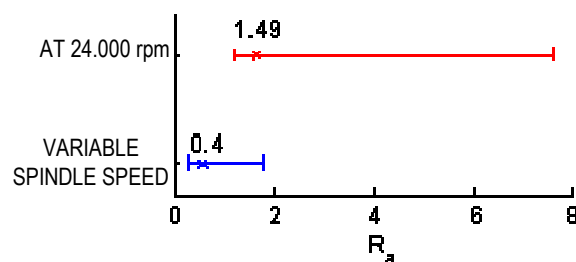

Figure 13. Mean R_a and standard deviation in microns for each test part.

Regarding the errors, little has been said about the uncertainty in the stability diagrams although several authors have recognized some inaccuracies [38]. Thevenot *et al.* [35] studied the influence of some input parameters on the stability diagram, showing that the critical parameter is the modal frequency of the system. For the method proposed here, the main sources of error in the stability diagram calculation come from the modelling of the process, the tool-path discretization and the input parameters.

The hypotheses assumed in the model for simplicity's sake introduce an error: the simplified non-trochoidal kinematic of the tool edges [39], the linear forces model or the relation between dynamic forces and dynamic displacements [40-42]. The stability algorithm can introduce an error in the solution, particularly if the single-frequency solution is used in interrupted milling. However, comparisons between analytical stability models and time domain models have demonstrated the poor influence of some of those hypotheses on the accuracy of the stability diagram in the lower order lobes area [43]. Hence, authors assume that the main source of error in the modelling in the present work comes from the averaging performed for the bull-nose end mill.

The tool-path is in this work discretized to study the variation of the modal parameters. However, in fact that variation is continuous. On the other hand, the variation of the modal parameters must influence the regenerative mechanism, delaying or facilitating the chatter appearance or the chatter stabilization. If spindle speed variation techniques distort the chip thickness regeneration varying the tooth passing frequency with respect to the natural frequency, the variation of the natural frequency with respect to the cutting frequency should have the same effect [44]. Another error comes from ignoring the feed speed. When the tool enters and leaves unstable areas in the diagram, the process needs some time to become unstable or stable. However, the discretization proposed assumes that both the chatter onset and the stabilization occur immediately, which is not really true. This error should affect the boundary of the unstable areas, making them vertically wider or narrower. It shouldn't affect horizontal width though, which is critical for the stable spindle speeds selection.

Another source of errors in the method proposed is related to the input parameters of the model. Leaving aside the wear of the tool edges or the variation of the radial depth of cut due to the tool deflection, which in this work have been avoided using a new tool for the experiments and minimizing the tool overhang, the main uncertainty is associated with the cutting coefficients and the modal parameters. The error in the characterization of the cutting coefficients for the forces model can be estimated in a 10% approximately. Considering the well-known relation between the critical depth of cut and the tangential shearing cutting coefficient, the influence of this error in the stability boundary has the same order [45].

The estimation of the modal parameters is not free of errors. If it is made experimentally, they come from the measurement and the modal fitting. Even using a low-weight accelerometer, the mass and the stiffness of the wire can influence the measurement of thin parts with high modal frequencies. Özsahin et al. [46] obtained errors of the 10% in the natural frequency of a tool with a diameter of 12 mm and an overhang of 80 mm because of a mass of 2,5 gr from the accelerometer. This error is critical as it has a proportional effect in the stability diagram displacing the lobes horizontally and distorting the stable speeds selection. If the modal parameters are obtained by FEM, the modal analysis depends on the quality of the model used. Nevertheless, the damping ratio is still needed and has to be calculated experimentally. Finally, the contact between the cutting edge and the workpiece also changes the modal parameters [47]. Although this effect has not been well studied, the engagement with the tool transitorily increases the dynamic stiffness of the part as it provides support and friction.

All these factors that distort the estimation of the stability diagrams illustrate the complexity of the milling of thin floors and the study of its stability and, instead of invalidating the methodology proposed, delimit the applications where the method can be used. Therefore, the method proposed is more reliable when the relation between the modal frequencies of the part and the tooth passing frequencies available is low, that is, when milling between the first lobes is possible and the stable areas are wide enough to be unaffected by the uncertainties mentioned.

7. Conclusions

In this work, a stability model of the milling of compliant systems in the tool axis direction with bull-nose end mills is combined with an analysis of the variation of the modal parameters of thin floors to provide stability diagrams that allow the selection of stable spindle speeds during the machining of thin floors. The main contributions of this work are:

- The averaging method proposed to take into account the variable cutting edge of the tool, which introduces nonlinearities in the stability algorithm because the cutting edge lead angle and the cutting coefficients are dependent on the axial depth of cut.
- The use of a stability diagram that relates the tool position along the tool-path with the spindle speed, allowing the selection of spindle speeds that avoid the unstable areas of the diagram.

The stability model solves the problem of the variation of the cutting edge lead angle and the cutting coefficients by means of an average of those values inside the dynamic chip volume, which is the responsible for the chatter occurrence. The solution takes into account the modal parameters to estimate whether the chip modulation occurs in the flank of the tool edge or in the toroidal part and, as a result, give more weight to the lead angle or the cutting coefficients values in those areas of the tool. This approach has been validated by means of cutting tests in a device that is compliant in the tool axis direction and has constant modal parameters. The 87% of the tests performed were in touch with reality and the main discrepancies were in the flank of the lobes that is more sensitive to the errors in the input parameters. Taking into account all the simplifications assumed in the model, the agreement seems reasonable.

Regarding the prediction of stability diagrams for thin floors milling, a FEM modal analysis is proposed in several intermediate steps of the machining, to consider the loss of mass and the tool position. Then, the stability model with the averaging is used to calculate the 3D stability diagrams. However, as the axial and radial depths of cut are already defined in the FEM model, the 3D diagram is simplified to a 2D diagram that relates spindle speed and tool position. This diagram indicates how the spindle speed must be varied along the tool-path. Also, the diagram not only defines boundary of the unstable areas but also how unstable can they be.

The procedure has been applied to the milling of a test part with a thin floor of 120x74 mm and a final thickness of 1 mm, and then compared with the milling of the floor at the maximum spindle speed of the machine. Even though the modal frequencies of the test part only allowed the selection of spindle speeds between the third to seventh order lobes, which can be a sensitive area, the variation of the spindle speed according to the

stability diagram has proven to improve the surface finish. Not only has been the mean R_a in the whole floor reduced from 1,49 μm to 0,4 μm, but also the deviation of the R_a values.

Regarding the uncertainty in the stability diagrams proposed, the main sources of inaccuracy in the prediction come from the modelling, the tool-path discretization and the input parameters of the model: cutting coefficients and modal parameters. The most critical is the error in the estimation of the modal frequency, as it proportionally distorts the location of the stable speeds. As a result, the method proposed is more reliable and should be considered as an alternative to other methods when the relation between the modal frequencies and the tooth passing frequencies allows milling above or between the low order lobes, so the stable areas are wide enough to be unaffected by the uncertainties. The tests with the thin floor were made in the region of the diagram between the third and the sixth order lobes. For higher order lobes, the location of the stable speeds becomes too sensitive to the input parameters.

Finally, although the procedure proposed has been used for the stability prediction of the milling of thin floors, it can be also used for the milling of thin walls, the turning of thin components or, in general, the machining of parts with variable modal parameters.

Acknowledgement

References

[1] W.R., Winfough, Issues of dynamics in high-speed milling of aluminum aircraft structures, Philosophical Dissertation, University of Florida, (1995).
[2] S., Smith, D., Dvorak, Tool path strategies for high speed milling aluminium workpieces with thin webs, Mechatronics 8 (1998) 291–300.
[3] F., Ismail, R., Ziaei, Chatter suppression in five-axis machining of flexible parts, International Journal of Machine Tools & Manufacture 42 (2002) 115-122.
[4] E., Budak, L. Kops, Improving productivity and part quality in milling of titanium based impellers by chatter suppression and force control, Annals of the CIRP 49/1 (2000) 31-32.
[5] C.M., Lee, S.W., Kim, K.H., Choi, D.W., Lee, Evaluation of cutter orientations in high-speed ball end milling of cantilever-shaped thin plate, Journal of Materials Processing Technology 140 (2003) 231-236.
[6] T., Aoyama, Y., Kakinuma, Development of Fixture Devices for Thin and Compliant Workpieces, Annals of the CIRP 54 (2005) 325-328.
[7] N.D., Sims, Y., Zhang, Piezoelectric active control for workpiece chatter reduction during milling, Smart Structures and Materials 2004: Smart Structures and Integrated Systems, Proc. of SPIE 5390 (2004) 335-346.
[8] Y., Altintas, M., Weck, Chatter stability of metal cutting and grinding, Annals of the CIRP 53 (2004) 619-652.
[9] Y., Altintas, E., Budak, Analytical prediction of stability lobes in milling, Annals of the CIRP 44 (1995) 357-362.

[10] E., Budak, Y., Altintas, Analytical prediction of the chatter stability in milling-Part I: General formulation, Journal of Dynamic Systems, Measurement and Control 120 (1998) 22–30.

[11] T., Insperger, B.P., Mann, G., Stépán, P.V., Bayly, Stability of up-milling and down-milling, part 1: Alternative analytical methods, International Journal of Machine Tools and Manufacture 43 (2003) 25-34.

[12] P.V., Bayly, J.E., Halley, B.P., Mann, M.A., Davies, Stability of interrupted cutting by temporal finite element analysis, Journal of Manufacturing Science and Engineering 125 (2003) 220–225.

[13] J., Gradisek, M., Kalveram, T., Insperger, K., Weinert, G., Stepan, E., Govekar, I., Grabec, On stability prediction for milling, International Journal of Machine Tool and Manufacture 45 (2005) 769–781.

[14] E.A., Butcher, H., Ma, E., Bueler, V., Averina, Z., Szabo, Stability of linear time-periodic delay-differential equations via Chebyshev polynomials, International Journal for Numerical Methods in Engineering 59 (2004) 895-922.

[15] M., Zatarain, J., Muñoa, G., Peigne, T., Insperger, Analysis of the influence of mill helix angle on chatter stability, Annals of the CIRP 55 (2006) 365-368.

[16] E., Budak, Mechanics and Dynamics of Milling Thin Walled Structures, PhD Thesis, University of British Columbia, Vancouver (1994).

[17] F., Lapoujoulade, T., Mabrouki, K., Raïssi, Prédiction du comportement vibratoire du fraisage latéral de finition des pièces à parois minces, Mécanique et Industrie 3 (2002) 403–418.

[18] V., Thevenot, L., Arnaud, G., Dessein, G., Cazenave-Larroche, Influence of material removal on the dynamic behaviour of thin walled structure in peripheral milling, Machining Science and Technology 10 (2006) 275–287.

[19] E., Budak, Y., Altintas, Analytical prediction of the chatter stability in milling - Part II: Application of the general formulation to common milling systems, Journal of Dynamic Systems, Measurement and Control 120 (1998) 31–36.

[20] O.B. Adetoro, W.M. Sim, P.H. Wen, An improved prediction of stability lobes using nonlinear thin wall dynamics, Journal of Materials Processing Technology 210 (2010) 969-979.

[21] I. Mañé, V. Gagnol, B.C. Bouzgarrou, P. Ray, Stability-based spindle speed control during flexible workpiece high-speed milling, International Journal of Machine Tools and Manufacture 48 (2008) 184-194.

[22] J.V., LeLan, A., Marty, J.F., Debongnie, Providing stability maps for milling operations, International Journal of Machine Tools and Manufacture 47 (2007) 1493-1496.

[23] U., Bravo, O., Altuzarra, L.N., López de Lacalle, J.A., Sanchez, F.J., Campa, Stability limits of milling considering the flexibility of the workpiece and the machine, International Journal of Machine Tools and Manufacture 45 (2005) 1669-1680.

[24] Z., Pan, H., Zhang, Z., Zhu, J., Wang, Chatter analysis of robotic machining process, Journal of Materials Processing Technology 173 (2006) 301-309.

[25] S.A., Jensen, Y.C., Shin, Stability analysis in face milling operation, Part - 1: Theory of stability lobe prediction, Journal of Manufacturing Science and Engineering 121 (1999) 600–605.

[26] A., Lamikiz, L.N., López de Lacalle, J.A., Sánchez, M.A., Salgado, Cutting force estimation in sculptured surface milling, International Journal of Machine Tools and Manufacture 44 (2004) 1511-1526.

[27] S., Engin, Y., Altintas, Mechanics and dynamics of general milling cutter. Part I: helical end mills, International Journal of Machine Tools and Manufacture 41 (2001) 2195-2212.

[28] Y., Altintas, Analytical prediction of three dimensional chatter stability in milling, The Japan Society of Mechanical Engineers, International Journal Series 44 (2001) 717–723.

[29] F., Abrari, M.A., Elbestawi, A.D., Spence, On the Dynamics of Ball End Milling: Modeling of Cutting Forces and Stability Analysis, International Journal of Machine Tools and Manufacture 38 (1998) 215-237.

[30] Y., Altintas, E., Shamoto, P., Lee, E., Budak, Analytical Prediction of Stability Lobes in Ball End Milling, Transactions of the ASME, Journal of Manufacturing Science and Engineering 121 (1999) 586-592.

[31] E. Ozlu, E. Budak, Comparison of one-dimensional and multi-dimensional models in stability analysis of turning operations, International Journal of Machine Tools and Manufacture 47 (2007) 1875-1883.

[32] F.J. Campa, L.N. López de Lacalle, A. Lamikiz, J.A. Sánchez, Selection of cutting conditions for a stable milling of flexible parts with bull-nose end mills, Journal of Materials Processing Technology 191 (2007) 279-282.

[33] O. Gonzalo, J. Beristain, H. Jauregi, C. Sanz, A method for the identification of the specific force coefficients for mechanistic milling simulation International Journal of Machine Tools and Manufacture 50 (2010) 765-774.

[34] S.D., Merdol, Y., Altintas, Multi Frequency Solution of Chatter Stability for Low Immersion Milling, Transactions of ASME, Journal of Manufacturing Science and Engineering 126 (2004) 459-466.

[35] V., Thevenot, L., Arnaud, G., Dessein, G., Cazenave-Larroche, Integration of dynamic behaviour in stability lobes method: 3D lobes construction and application to thin walled structure milling, International Journal of Advanced Manufacturing Technology 27 (2006) 638–644.

[36] D.J., Ewins, Modal testing theory, practice and application, 2nd Edition, Research Studies Press LTD. (2000).

[37] F. J., Campa, S., Seguy, L. N., López de Lacalle, L., Arnaud, G., Dessein, G., Aramendi, Stable Milling of Thin-Walled Parts with Variable Dynamics, Proc. of the 6th International Conference on High Speed Machining, San Sebastian (2007).

[38] M., Weck, Handbook of machine tools. Vol.4. Metrological analysis and performance test, John Wiley & Sons (1984).

[39] X.-H., Long, B., Balachandran, B.P., Mann, Dynamics of milling processes with variable time delays, Nonlinear Dynamics 47 (2007) 49-63.

[40] C. Brecher, M. Esser, S. Witt, Interaction of manufacturing process and machine tool, CIRP Annals - Manufacturing Technology 58 (2009) 588-607.

[41] Y. Altintas, M. Eynian, H. Onozuka, Identification of dynamic cutting force coefficients and chatter stability with process damping, CIRP Annals-Manufacturing Technology 57 (2008) 371-374.

[42] I., Minis, R., Yanushevsky, A., Tembo, Analysis of linear and nonlinear chatter in milling, Annals of the CIRP 39 (1990) 459-462.

[43] Y. Altintas, G. Stepan, D. Merdol, Z. Dombovari, Chatter stability of milling in frequency and discrete time domain, CIRP Journal of Manufacturing Science and Technology 1 (2008) 35-44.

[44] M. Zatarain, I. Bediaga, J. Muñoa, R. Lizarralde, Stability of milling processes with continuous spindle speed variation: Analysis in the frequency and time

domains, and experimental correlation, CIRP Annals-Manufacturing Technology 57 (2008) 379-384.

[45] Y., Altintas, Manufacturing Automation, Cambridge University Press, Cambridge, MA, (2000).

[46] O., Özsahin, H.N., Özgüven, E., Budak, Analysis and compensation of mass loading effect of accelerometers on tool point FRF measurements for chatter stability predictions, International Journal of Machine Tools and Manufacture 50 (2010) 585-589.

[47] O., Gonzalo, G., Peigné, D., González, High speed machining simulation of thin-walled components, 5th International Conference on High Speed Machining, Metz, (2006).